Science of the Total Environment 824 (2022) 153708

Contents lists available at ScienceDirect

Science of the Total Environment

journal homepage: www.elsevier.com/locate/scitotenv

Ambient observations indicating an increasing effectiveness of ammonia control in wintertime $PM_{2.5}$ reduction in Central China

Mingming Zheng [a,b,c], Yuhang Wang [c,*], Lianxin Yuan [d], Nan Chen [d], Shaofei Kong [b,*]

[a] School of Chemical and Environmental Engineering, Wuhan Polytechnic University, Wuhan 430023, China
[b] School of Environmental Studies, China University of Geosciences (Wuhan), Wuhan 430074, China
[c] School of Earth and Atmospheric Sciences, Georgia Institute of Technology, Atlanta, GA, USA
[d] Hubei Environment Monitoring Center, Wuhan 430072, China

HIGHLIGHTS

- Increasing effectiveness of ammonia control is found in wintertime $PM_{2.5}$ reduction.
- Emission reduction selection is based on critical total ammonia concentration.
- SO_2 + NO_x remains the preferred way to reduce inorganic $PM_{2.5}$ in Central China.

GRAPHICAL ABSTRACT

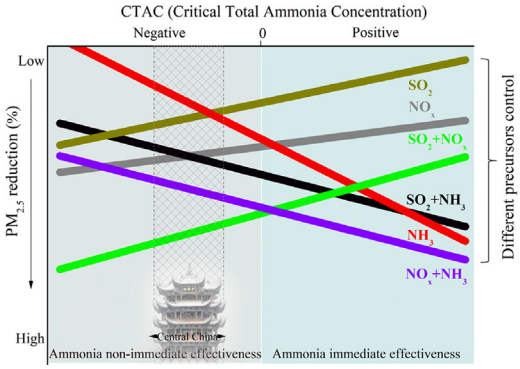

ARTICLE INFO

Article history:
Received 6 January 2022
Received in revised form 2 February 2022
Accepted 2 February 2022
Available online 16 February 2022

Editor: Pingqing Fu

Keywords:
Emission reduction
Inorganic particles
Effectiveness
Critical total ammonia concentration

ABSTRACT

Ammonia emission reduction is increasingly being considered one of the control measures to mitigate wintertime fine particulate matter ($PM_{2.5}$) pollution. Three wintertime observations from 2012 to 2018 in Wuhan, China, were analyzed to examine the effectiveness of ammonia control in wintertime $PM_{2.5}$ reduction based on the critical total ammonia concentration (CTAC, i.e., the inflection point of effective ammonia control for $PM_{2.5}$ mass reduction based on the asymmetric response of $PM_{2.5}$ to ammonia control). The CTAC gradually approached 0% (immediate effectiveness), with values of −26% in 2012, −23% in 2015, and −9% in 2018. At the observed ambient conditions, there were significant positive correlations of the CTAC with sulfate and total nitrate changes, in contrast to the negative correlation of the CTAC with total ammonia change. An approximately 10% total ammonia reduction could offset the decline in CTAC attributed to a 30–40% sulfate or 20–30% total nitrate reduction in Wuhan. This study indicates that the combined control of SO_2 + NO_x ($NO+NO_2$) remains the preferred way to reduce inorganic particles in Central China at present, despite a tendency of the ambient chemical state moving towards effective ammonia control. However, as the CTAC approaches 0%, the effectiveness of ammonia and NO_x reduction measures targeting wintertime $PM_{2.5}$ can greatly exceed that observed during the 2012–2018 period in Central China.

1. Introduction

With the continuous demand for fine particulate matter ($PM_{2.5}$) reduction (Zhou et al., 2022; An et al., 2019; Bai et al., 2019), there is increasing concern regarding ammonia control (Gu et al., 2021; Ma et al., 2021; Liu et al., 2019), due to its role as a precursor in particle formation (Cheng

* Corresponding authors.
E-mail addresses: yuhang.wang@eas.gatech.edu (Y. Wang), kongshaofei@cug.edu.cn (S. Kong).

http://dx.doi.org/10.1016/j.scitotenv.2022.153708

et al., 2021; Chu et al., 2019; Behera and Sharma, 2010). The main concern is the realization of effective emission control to improve the air quality (Plautz, 2018). Previous studies have demonstrated the necessity of ammonia abatement in fine particulate matter reduction in the United States (Pinder et al., 2007) and Europe (Backes et al., 2016). However, the uncertainty surrounding the effectiveness of ammonia control has remained and resulted in regulators in China not formulating or implementing ammonia emission control policies and measures (Fu and Chen, 2017).

$PM_{2.5}$ pollution can be affected by ammonia emissions (An et al., 2019; Liu et al., 2019; Wu et al., 2016). An increase in the ammonium concentration can reduce the benefits of secondary inorganic aerosol concentration reduction resulting from SO_2 and NO_x emission control (Fu et al., 2017). Wang et al. (2011) indicated that the nitrate concentration was sensitive to ammonia emissions in the Pearl River Delta, while the nitrate concentration was more sensitive to NO_x emissions in the North China Plain and Yangtze River Delta. Guo et al. (2018) suggested that the effect of NH_x (total ammonia; $NH_x = NH_3 + NH_4^+$) control in terms of inorganic $PM_{2.5}$ reduction in Beijing was not as notable as that of TNO_3 ($TNO_3 = NO_3^- + HNO_3$) and SO_2 control unless the NH_x reduction degree exceeded 60%. In contrast to the United States or Europe, there occurs a higher $PM_{2.5}$ concentration in China (Wang et al., 2017; Cao, 2012), especially in winter (Yang et al., 2016; Cao et al., 2012), and a higher atmospheric ammonia concentration (Zhang et al., 2017; Huang et al., 2012). It is necessary to explore the effectiveness of ammonia emission control in terms of $PM_{2.5}$ reduction and scientifically formulate emission control strategies.

Previous studies have noted that the effect of ammonia control on inorganic particulate matter depends on the aerosol thermodynamic equilibrium between the total ammonia and the sum of the total nitrate and net negative charge excluding H^+ and NH_4^+ (Zheng et al., 2019). Xu et al. (2019) defined the molar ratio between these two terms as *R*, and Blanchard et al. (2000) defined the difference between these two terms as the excess NH_3 (please refer to supporting information for details). In regard to *R* and excess NH_3, the theoretical indicators values for NH_x partition transition are 1 and 0, respectively (Xu et al., 2019; Blanchard et al., 2000). In addition, Guo et al. (2018) proposed that effective NH_3 control occurs at particulate pH values below 3. Zheng et al. (2019) analyzed the asymmetric responses of the particulate mass to ammonia emissions and defined the critical total ammonia concentration (CTAC), which is the inflection point of effective ammonia control for inorganic particulate mass reduction. The CTAC value of −25% reported in Zheng et al. (2019) implied that only after NH_x reduction exceeds 25% can ammonia control effectively reduce the inorganic $PM_{2.5}$. In that study, the CTAC point correspond to the condition in which the NH_x molar concentration was not equal to but 40–50% higher than the sum of TNO_3 and the net negative charge excluding H^+ and NH_4^+.

With three datasets of wintertime observations of the hourly water-soluble inorganic ions in $PM_{2.5}$ and precursor gases in 2012, 2015 and 2018 in Wuhan, the variation in $PM_{2.5}$ chemical components was elucidated. These periods corresponded to the periods before, during and after the implementation of the Air Pollution Prevention and Control Action Plan in China, respectively. With the use of the CTAC concept, the changes of the effectiveness of ammonia emission control on inorganic particle mitigation from 2012 to 2018 were analyzed using a thermodynamic model. Furthermore, we estimated the impact of sulfate, total nitrate and ammonia changes on the CTAC and quantified their relationship. Finally, the effects of emission control measures (including SO_2, NO_x, and NH_3 and their combinations) on $PM_{2.5}$ reduction as a function of the CTAC were examined.

2. Materials and methods

2.1. Observations

The observation site (114.36°N, 30.53°E) is located in a representative mixed commercial/residential area with no nearby industrial emissions in Wuhan, a megacity in Central China (Fig. 1). Water-soluble ions including Cl^-, NO_3^-, SO_4^{2-}, NH_4^+, Na^+, Mg^{2+}, K^+, and Ca^{2+} in $PM_{2.5}$ and gaseous NH_3, HNO_3 and HCl were synchronously observed with an online ion chromatography analyzer at a 1-h resolution (MARGA-ADI 2080) (Li et al., 2019; Zheng et al., 2019). Relevant quality assurance (QA)/quality control (QC) procedures have been reported in our previous studies (Zheng et al., 2019). Three wintertime observation campaigns (three cases) were performed from 2012 to 2018. Case 1 lasted from December 16, 2012, to January 24, 2013. Case 2 ranged from December 1, 2015, to January 21, 2016. Case 3 extended from December 1, 2018, to January 30, 2019. These three cases encompassed a total of 120 days, and the number of effective hours per day reached at least 20 h. Hourly $PM_{2.5}$, SO_2 and NO_2 concentrations were synchronously monitored with β-ray, ultraviolet fluorescence and chemiluminescence online monitoring equipment, respectively (Zheng et al., 2019), except for December 2012 due to instrument installation. Meteorological parameter data, including relative humidity (RH), ambient temperature (T), wind speed and direction, and precipitation were obtained from the local observatory.

2.2. Simulations

The thermodynamic ISOROPPIA-II model (http://nenes.eas.gatech.edu/ISORROPIA) (Fountoukis and Nenes, 2007; Nenes et al., 1998) was adopted to predict the existing form of species (gas or aerosol phase) and calculate their concentrations under chemical equilibrium, with inputs of Cl^-, NO_3^-, SO_4^{2-}, NH_4^+, Na^+, Mg^{2+}, K^+, Ca^{2+}, ambient RH, T, and gaseous precursors (HNO_3, HCl and NH_3) (Song et al., 2018; Murphy et al., 2017). Following previous studies (Guo et al., 2016; Weber et al., 2016; Guo et al., 2015; Hennigan et al., 2015), this work is based on the observed concentrations and the effects of transport and deposition were not considered, although ~70% of the observations were taken with wind speed <2 m s^{-1}. The forward mode with metastable state was applied due to its better performance and more accurate and robust results (Guo et al., 2016; Weber et al., 2016; Guo et al., 2015; Hennigan et al., 2015; Fountoukis and Nenes, 2007). The observed lowest RH reached 25.6%, which meets the model operation assumption that the considered inorganic ions occur in the aqueous phase (Guo et al., 2017; Bertram et al., 2011; Fountoukis and Nenes, 2007; Ansari and Pandis, 2000). The concentrations of the inorganic components (SO_4^{2-}, NO_3^- and NH_4^+) predicted with the ISOROPPIA-II model coincided well with the corresponding measured concentrations (Fig. S1).

In Section 3.2, which describes CTAC sensitivity simulations, the input SO_4^{2-}, TNO_3 or NH_x concentrations were subject to interannual replacement. For instance, the average input SO_4^{2-} concentration in 2012 was replaced by the average concentration in 2015. In summary, the hourly SO_4^{2-} concentration in 2012 was multiplied by the average SO_4^{2-} concentration ratio between 2015 and 2012, with the other model inputs unchanged. The same simulation approach was applied to both TNO_3 and NH_x and the chemical components in 2015.

3. Results and discussion

3.1. Variation in wintertime inorganic components from 2012 to 2018

The three wintertime episodes were characterized by high levels of $PM_{2.5}$ and inorganic components. Although the SNA (SO_4^{2-}, NO_3^- and NH_4^+) concentrations were decreased from 2012 to 2018 (Table 1), their fractions in $PM_{2.5}$ gradually increased, with total average fractions of 51.3%, 62.9% and 63.8%, respectively. Secondary inorganic particles comprise the dominant components of $PM_{2.5}$ under wintertime pollution conditions in Central China, similar to a previous study (Zheng et al., 2019), and the SNA fraction increases are attributed possibly to the increasing atmospheric oxidation (Fig. S5, Table 1) (Fu et al., 2020; Zhang et al., 2020; Wang et al., 2019) and decreasing primary $PM_{2.5}$ emissions (Zhang et al., 2019).

The changes in SO_4^{2-}, TNO_3 and NH_x from 2012 to 2018 are shown in Fig. 2. SO_4^{2-} and NH_x decreased, while TNO_3 notably increased by 30.2% after a slight decrease. In the low-concentration quartile, the SO_4^{2-}

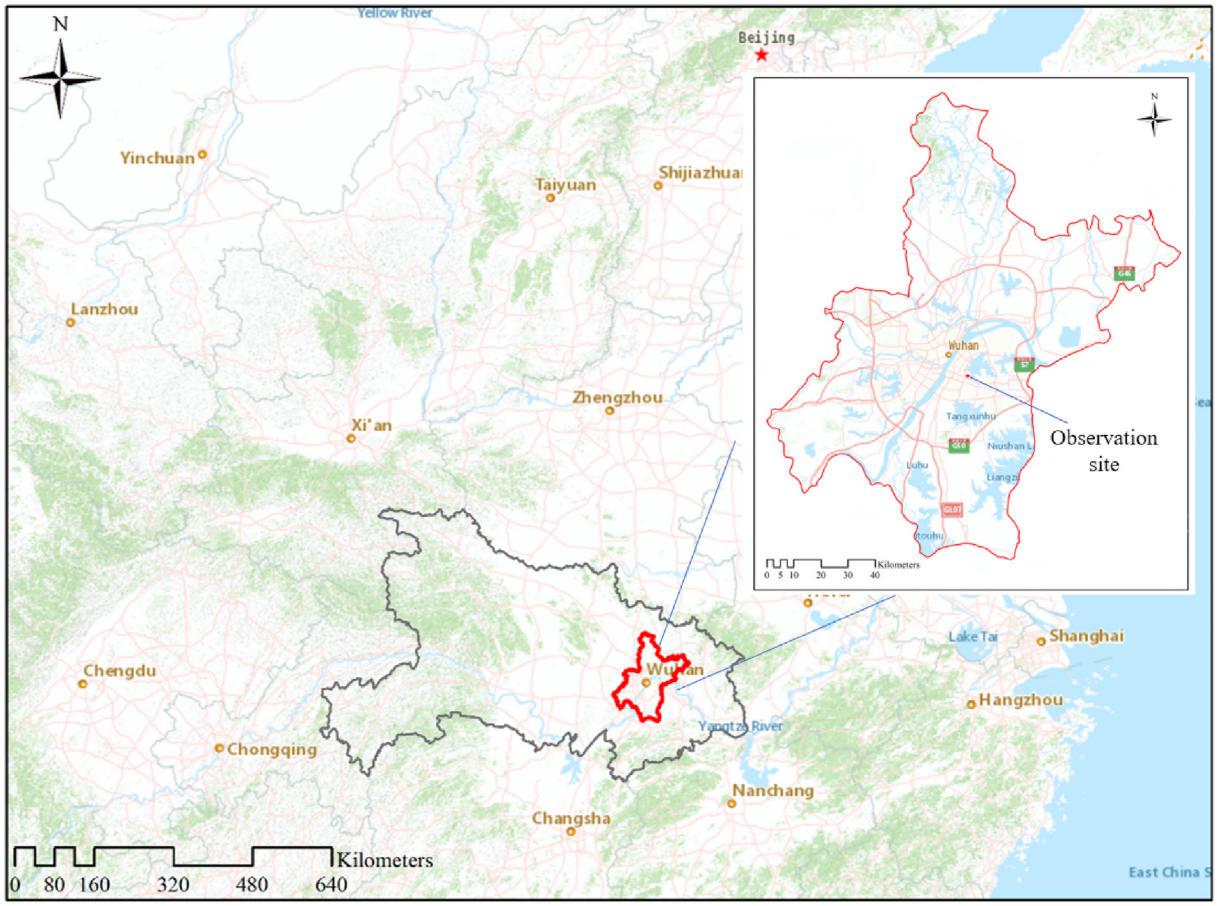

Fig. 1. Location of Wuhan, Hubei Province in China.

frequency significantly increased by 200%, while TNO_3 exhibited a 40% decrease from 2012 to 2018. In contrast, the frequency of high SO_4^{2-} concentrations largely decreased by 88%, but the high TNO_3 concentration quartile obviously increased by 86%. More attention should be paid to wintertime high-TNO_3 concentration days in the future. In regard to NH_x, the fourth high-concentration quartile decreased by 57% from 2012 to 2018, while there was no obvious increase in the low-concentration quartile, indicating a decrease in high-concentration emissions in past and nonnegligible low-concentration days under ammonia control.

The SO_4^{2-} reduction from 2012 to 2018 was mainly attributed to effective SO_2 emission control (Jin et al., 2016) (Fig. S2). Gradually decreasing ammonia emissions mainly from agriculture (Fig. S3) in the observed region were beneficial to NH_x reduction (Pinder et al., 2008). Except for a decline in fertilizer application (Das et al., 2009) (Fig. S4), the Chinese government announced the plan of "Resource Utilization of Livestock and Poultry Waste" (China State Council, 2017) in June 2017, which may have also facilitated a decrease in ammonia emissions. Atmospheric NO and NO_x continuously decreased from 2012 to 2018, while NO_2 rebounded by 18.5% in 2018 (Fig. S5) due in part to the increasing atmospheric oxidation resulting from a nearly doubled NO_2/NO ratio from 2015 to 2018 (Fig. S5). The growing NO_2 benefited to increase HNO_3 and formed nitrate (Seinfeld and Pandis, 2006).

Table 1
Statistic of the mass concentrations, species proportions and meteorological parameters in the three winters in Wuhan.

	Case 1 (Winter 2012)	Case 2 (Winter 2015)	Case 3 (Winter 2018)
SNA ($\mu g\ m^{-3}$)	79.2 ± 40.6	67.6 ± 45.1	62.0 ± 33.6
O_3 ($\mu g\ m^{-3}$)[a]	22.1 ± 27.6	26.0 ± 23.4	27.6 ± 24.9
$SO_4^{2-}/PM_{2.5}$ (%)	19.1 ± 6.4	21.2 ± 7.7	11.3 ± 8.0
$NO_3^-/PM_{2.5}$ (%)	19.1 ± 4.8	26.0 ± 8.4	36.5 ± 18.2
$NH_4^+/PM_{2.5}$ (%)	13.1 ± 3.1	15.8 ± 4.4	16.0 ± 6.0
NO_x/SO_2[b]	4.58 ± 3.24	8.97 ± 7.84	10.9 ± 11.5
RH (%)	79.5 ± 16.8	79.8 ± 19.4	79.2 ± 15.9
T (K)	276.9 ± 3.13	280.0 ± 3.07	279.6 ± 3.62

SNA: including sulfate, nitrate and ammonium.
RH: relative humidity.
T: temperature.
[a] Hourly concentration in January.
[b] Molar concentration ratio in atmosphere, NO_x including NO and NO_2.

3.2. Approaching effective wintertime ammonia control in $PM_{2.5}$ reduction from 2012 to 2018

The responses of the total water-soluble ions (WSIs, including NH_4^+, NO_3^-, SO_4^{2-}, HSO_4^-, Cl^-, Na^+, K^+, Ca^{2+} and Mg^{2+}) to NH_x changes are shown in Fig. 3. These WSIs exhibited logarithmic responses to NH_x variation, consistent with a previous study (Zheng et al., 2019). With an increase/decrease of 80% in NH_x, these WSIs changed by +0.22%/−48.4%, +0.44%/−52.0%, and +1.93%/−63.3% during the winters of 2012, 2015 and 2018, respectively.

The transition in the WSIs response from fast to slow was explored, at 1% NH_x intervals. The CTAC where the absolute value of the second-order derivative reached a maximum was regarded as the inflection point of the WSIs response to ΔNH_x. During winters of 2012, 2015 and 2018, the CTAC values were −26%, −23% and −9%, respectively, corresponding to required NH_x reduction of 6.56, 5.03 and 1.82 $\mu g\ m^{-3}$, respectively, before reaching the inflection point. The variation in CTAC indicated a declining need to reduce NH_x before the effectiveness of ammonia control in terms of $PM_{2.5}$ reduction could be realized.

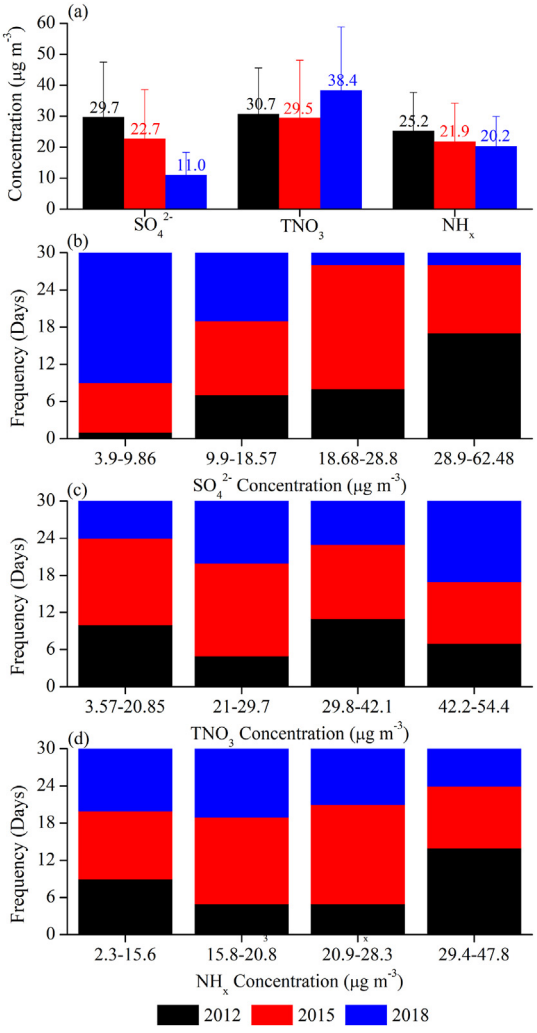

Fig. 2. Concentration changes in SO_4^{2-}, TNO_3 and NH_x and the daily frequency by the quartile in winters of 2012, 2015 and 2018.

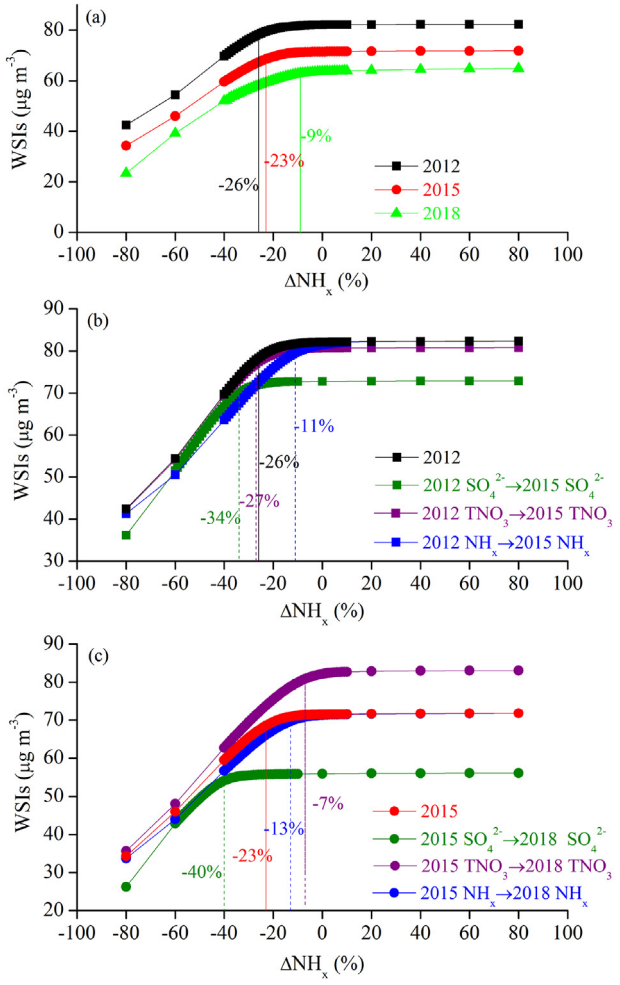

Fig. 3. Changes in the WSIs as a function of ΔNH_x. The vertical lines indicate the CTAC during the three winter episodes (a), replacing the average SO_4^{2-}, TNO_3 and NH_x concentrations in 2012 with those in 2015 (b) and replacing the average SO_4^{2-}, TNO_3 and NH_x concentrations in 2015 with those in 2018 (c).

To further examine the driving factors of the CTAC, the CTAC sensitivity was evaluated corresponding to the observed changes in SO_4^{2-}, TNO_3 or NH_x from 2012 to 2015, and from 2015 to 2018 (please refer to Section 2.2 for details). The corresponding responses of the considered WSIs are shown in Fig. 3. The CTAC changed from −26% to −34%, and from −23% to −40%, respectively, with the SO_4^{2-} in 2012 and 2015 replaced by those in 2015 and 2018, respectively. Regarding TNO_3 substitution, compared to 2012–2015 and 2015–2018, the CTAC changed by −1% and +16%, respectively. In regard to NH_x replacement in 2012 and 2015, the CTAC increased from −26% to −11%, and from −23% to −13%, respectively. In contrast to NH_x, the increase in SO_4^{2-} and TNO_3 resulted in an increase in the CTAC value. The cumulative results for SO_4^{2-}, TNO_3 and NH_x substitution ($\Delta CTAC_{Total}$) were generally consistent with the CTAC changes determined based on the observation data ($\Delta CTAC_{Actual}$) (Table S1), indicating that SO_4^{2-}, TNO_3 and NH_x were the key factors influencing the effectiveness of ammonia control on $PM_{2.5}$ reduction. The difference between $\Delta CTAC_{Total}$ and $\Delta CTAC_{Actual}$ within 5% mainly attributed to the cumulative deviation in the linear relationship (Fig. 4).

Preliminary exploration revealed that the changes in SO_4^{2-} and TNO_3 within ±80% nearly imposed a linear impact on ΔCTAC (Fig. 4), with the CTAC decreasing by 3–4% and 3–7%, respectively, corresponding to a 10% reduction in the mass concentration. TNO_3 reduction in 2018 caused a larger decline in $\varepsilon(NH_4^+)$ (particulate NH_4^+ fraction, $\varepsilon(NH_4^+) = NH_4^+/NH_x$) (Fig. S6), with greater NH_x partitioning into the gas phase than that under SO_4^{2-} control, resulting in more ammonia control required to reduce $PM_{2.5}$ under the former control measure.

Further regression analysis between the CTAC and SO_4^{2-}, TNO_3 and NH_x mass concentrations was conducted. The CTAC responses to the SO_4^{2-}, TNO_3 or NH_x mass concentration at 20% change steps were considered, except for the extremely low SO_4^{2-} concentration such as a reduction over 80%. A total of 67 datasets verified the linear relationships between the CTAC and SO_4^{2-}, TNO_3, and NH_x concentrations. The equation was fitted as:

$$CTAC = 0.011[SO_4^{2-}] + 0.014[TNO_3] - 0.039[NH_x] \quad (R^2 = 0.92, p<0.001) \quad (1)$$

or

$$[CTAC] = 0.28[SO_4^{2-}] + 0.36[TNO_3] - [NH_x] \quad (R^2 = 0.98, p<0.001), \quad (2)$$

where CTAC in Eq. (1) is in the unit of % and [CTAC] in Eq. (2) is in the unit of μg m^{-3}. $[SO_4^{2-}]$, $[TNO_3]$ and $[NH_x]$ are sulfate, total nitrate and total ammonia mass concentrations (μg m^{-3}), respectively. A positive CTAC or [CTAC] value indicates that ammonia reduction can be directly implemented to effectively reduce $PM_{2.5}$. In contrast, a negative CTAC or [CTAC] value suggests that there is an initial cost of ammonia reduction that does not reduce inorganic $PM_{2.5}$ until the reduction of $[NH_x]$ reaches [CTAC].

Eqs. (1) and (2) indicated that the CTAC changes were more sensitive to changes in the NH_x mass concentration than to SO_4^{2-} and TNO_3 mass concentration changes, consistent with the substitution-based simulation

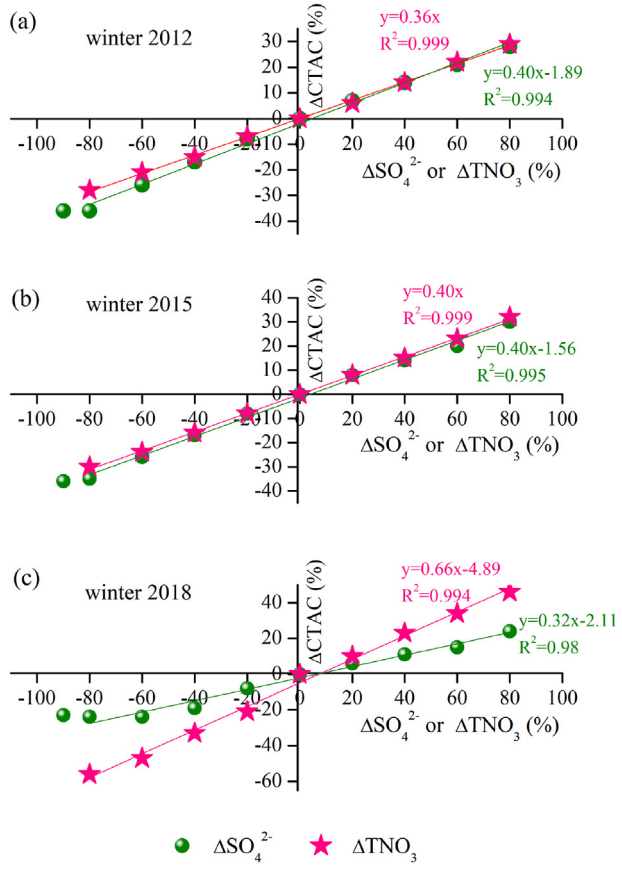

Fig. 4. CTAC changes as a function of SO_4^{2-} and TNO_3 variations relative to the baseline results with no SO_4^{2-} or TNO_3 reduction during the three winter episodes.

results listed in Table 2. For example, changes of 11.7 μg m^{-3} SO_4^{2-}, 8.9 μg m^{-3} TNO_3 and 3.3 μg m^{-3} NH_x led to similar amplitudes of CTAC changes (15–17%, corresponding to a [CTAC] value ranging from 3.5–3.7 μg m^{-3}; please refer to Table 2). This suggested that approximately 10% total ammonia reduction could offset the decline in CTAC attributed to a 30–40% sulfate or 20–30% total nitrate reduction.

3.3. Emission reduction measures based on the CTAC

Although effective ammonia control is increasingly accomplished from 2012 to 2018, the most effective $PM_{2.5}$ reduction method should be further confirmed. Here, we evaluate the relative effectiveness of individual SO_2, NO_x, and NH_3 control and their joint control measures in regard to $PM_{2.5}$ mitigation as a function of the CTAC with a thermodynamic model, thereby adopting an emission control ratio of 20% during the three winter periods. Variations in $PM_{2.5}$ are evaluated under achieved changes in SO_4^{2-}, TNO_3, and NH_x, representing SO_2, NO_x, and NH_3 emission control measures (Guo et al., 2018), respectively. The effect of various emission control measures on $PM_{2.5}$ reduction as a function of the CTAC is shown in Fig. 5.

Table 2
The changes of concentrations, CTAC and its corresponding mass concentration in response to the substitute of SO_4^{2-}, TNO_3 or NH_x from 2012 to 2015, and from 2015 to 2018, respectively.

		ΔConcentrations		ΔCTAC	Δ[CTAC] (μg m^{-3})
SO_4^{2-}	2012–2015	−7 μg m^{-3}	−23.6%	−8%	−2.02
	2015–2018	11.7 μg m^{-3}	−51.5%	−17.0%	−3.72
TNO_3	2012–2015	−1.2 μg m^{-3}	−3.9%	−1%	−0.25
	2015–2018	+8.9 μg m^{-3}	+23.2%	+16.0%	+3.50
NH_x	2012–2015	−3.3 μg m^{-3}	−13.1%	+15.0%	+3.78
	2015–2018	−1.7 μg m^{-3}	−7.8%	+10.0%	+2.19

Combined SO_2 + NO_x control was generally the most effective $PM_{2.5}$ reduction measure when the CTAC was lower than zero. The CTAC value corresponding to the observed winters ranged from −26% to −9%, as marked in the shaded areas in Fig. 5. This suggests that SO_2 + NO_x control measures can currently be implemented to optimally achieve wintertime $PM_{2.5}$ reduction in Central China. SO_2 or NO_x reduction can decrease ammonium due to ammonia gas-particle phase partitioning affected by the aerosol pH (Fig. S7), while NH_3 control mainly reduces gaseous ammonia under ammonia-rich conditions (Guo et al., 2018; Blanchard et al., 2000). For example, in 2018, a 20% reduction in NH_x decreased ammonium by approximately 6.3%, while total nitrate and sulfate reduction decreased ammonium by approximately 14.5% and 5.0%, respectively. In addition, changes in sulfate basically imposed no effect on particulate nitrate in this abundant ammonia system (Fig. S8) (Dennis et al., 2008). The average $PM_{2.5}$ concentration in the winter of 2018 reached 97.2 μg m^{-3}, exceeding the standard limit of 75 μg m^{-3} by 22.8% if the daily average standard were adopted. Fig. 5 indicates that it is necessary to strengthen emission control, e.g., a greater than 20% reduction in SO_2 + NO_x, so that the $PM_{2.5}$ concentration may reach the standard.

After reaching the CTAC, the effectiveness of ammonia control in terms of $PM_{2.5}$ reduction gradually increased. The combination of NO_x + NH_3 is the best $PM_{2.5}$ reduction approach at a CTAC value ranging from approximately 0–60%, as shown in Fig. 5. In this ammonia-poor system, NH_3 or NO_x reduction can effectively reduce ammonium and nitrate, as their reduction can result in the release of associated ammonia or nitric acid (Dennis et al., 2008; Blanchard et al., 2000). For instance, at a CTAC value higher than 30%, not only an approximately 20% particulate ammonium reduction but also an approximately 20% nitrate reduction can be achieved via a 20% NH_3 reduction. We can further speculate that NH_3 emission control alone can be comparable to joint NO_x + NH_3 control based on the higher linear slope of the former impact, specifically at CTAC value larger than 60%. When the CTAC is larger than 23%, it is worth noting that NH_3 emission control alone is more effective for $PM_{2.5}$ reduction than joint SO_2 + NO_x control. Sulfate reduction releases ammonia to react with nitric acid and potentially increases nitrate at CTAC values larger than zero due to the relative ammonia-poor conditions (Dennis et al., 2008; Blanchard et al., 2000). Therefore, it is not highly advisable to reduce $PM_{2.5}$ by decreasing SO_2 at positive CTAC values, except for SO_2 and NH_3 joint reduction for inorganic $PM_{2.5}$ reduction target within 10% at CTAC values higher than 18%.

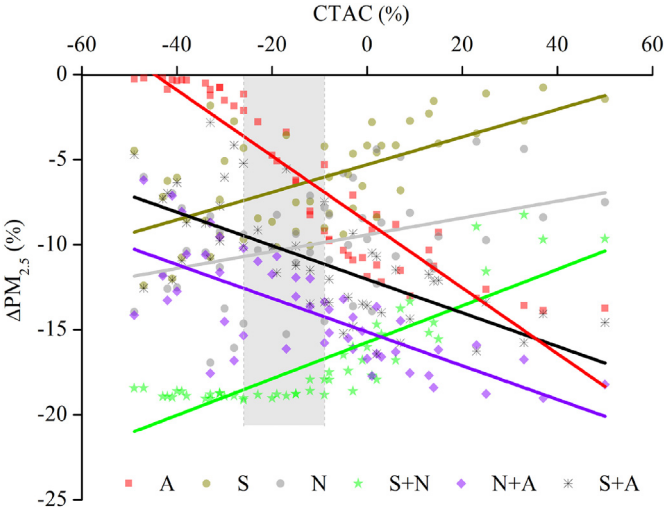

Fig. 5. Changes in $PM_{2.5}$ with the reduction in SO_4^{2-} (S), TNO_3 (N), NH_x (A) and their combinations as a function of the CTAC, adopting a reduction ratio of 20% in the winters as an example. "S + N" indicates that both SO_4^{2-} and TNO_3 are reduced by 20%. The shaded areas correspond to the observed winter periods in Central China.

Four control ratios, i.e., 10%, 20%, 30% and 50%, were further employed to verify the effect of the above emission reduction measures (Fig. 6). At any reduction ratio, the SO_2 + NO_x combination currently constitutes the most effective way to reduce inorganic $PM_{2.5}$ in Central China, with a 1.54–16.3% greater WSIs reduction than that achieved by the NO_x + NH_3 combination. With increasing reduction ratio, the advantage of SO_2 + NO_x over NO_x + NH_3 in terms of particle pollution mitigation increased (Fig. S9). The achieved decrease in $[NH_4^+]$ via SO_2 + NO_x joint reduction was 1.73–15.3% larger than that achieved by NO_x + NH_3 joint reduction, although the former scheme did not reduce ammonia emissions (Fig. S10). The SO_2 + NO_x reduction combination resulted in NH_x partitioning into the gas phase due to $\varepsilon(NH_4^+)$ decreased (Fig. S11). The NO_x + NH_3 combination notably increased $\varepsilon(NH_4^+)$, thereby promoting the conversion of ammonia into ammonium (Fig. S11). In addition, since SO_4^{2-} is nonvolatile, the SO_2 + NO_x combination could effectively reduce sulfate (Fig. S10).

Additionally, a comparison of the WSIs mitigation effect between SO_2 + NO_x and SO_2 + NO_x + NH_3 combinations is shown in Fig. S12. Regardless of the proportion of emission reduction, the latter scheme attained no obvious advantage over the former scheme because ammonium under the former scenario had already been partitioned into the gas phase under pH increase even though no NH_x reduction had occurred.

4. Implications

We made use of the wintertime observations in Wuhan in 2012, 2015, and 2018 to examine the effectiveness of ammonia reduction control. The thermodynamic equilibrium calculation was applied to compute the corresponding CTAC values, at which points the ammonia control becomes effective. As in a previous study (Zheng et al., 2019), all CTAC points were lower than the observed ammonia levels, implying that inorganic $PM_{2.5}$ concentrations were insensitive to the initial reduction of ammonia. As the observed concentrations of SO_4^{2-} and NH_x decreased from 2012 to 2018, the CTAC points moved closer to the observed ammonia level. In comparison, the observed TNO_3 concentrations did not decrease from 2012 to 2018. We attributed the observed decreases of SO_4^{2-} and NH_x and the general improvements of air quality in China (Zhang et al., 2019; Geng et al., 2019; Cheng et al., 2019; Geng et al., 2017) to emission reductions (Zheng et al., 2018; Jin et al., 2016; Zhao et al., 2013; China State Council, 2013, 2018). However, transport and deposition processes also affect SO_4^{2-} and NH_x concentrations, which were not considered in this study and might lead to uncertainties. Nonetheless, the observed chemical state of the atmosphere implies that the initial barrier of ammonia control decreased from 2012 to 2018 (Fig. 3) and the partition of TNO_3 shifted slightly from particulate towards gas phase (Fig. S6) in Wuhan.

Model sensitivity analysis indicated the sensitivity of CTAC to NH_x change differ from those of SO_4^{2-} and TNO_3. A reduction of NH_x tends to increase CTAC, making ammonia control more effective. In contrast, a reduction of SO_4^{2-} or TNO_3 tends to decrease CTAC, making ammonia control less effective. For example, a 10% reduction in SO_4^{2-} and TNO_3 led to decreases of 3%–4% and 3%–7%, respectively, in the CTAC. An approximately 10% total ammonia reduction could offset the decline in CTAC attributed to a 30–40% sulfate or 20–30% total nitrate reduction.

With the further requirements for air quality improvement (An et al., 2019; Fu and Chen, 2017; Li and Zhang, 2014), many studies have proposed the implementation of ammonia control measures to reduce $PM_{2.5}$ (An et al., 2019; Wu et al., 2016). We note that many factors, such as the abatement cost (Gu et al., 2021), acid rain (Liu et al., 2019), ozone collaborative control (Ou et al., 2022), health impacts (Ma et al., 2021), and nitrogen deposition (Pan et al., 2021), need to be considered in the decision-making process. These factors were not considered in this study. We highlight the fact that the efficiency of ammonia control in reducing $PM_{2.5}$ differs from those due to the emission control of SO_2. The effect of the latter is immediate and corresponds nearly to the emission reduction magnitude.

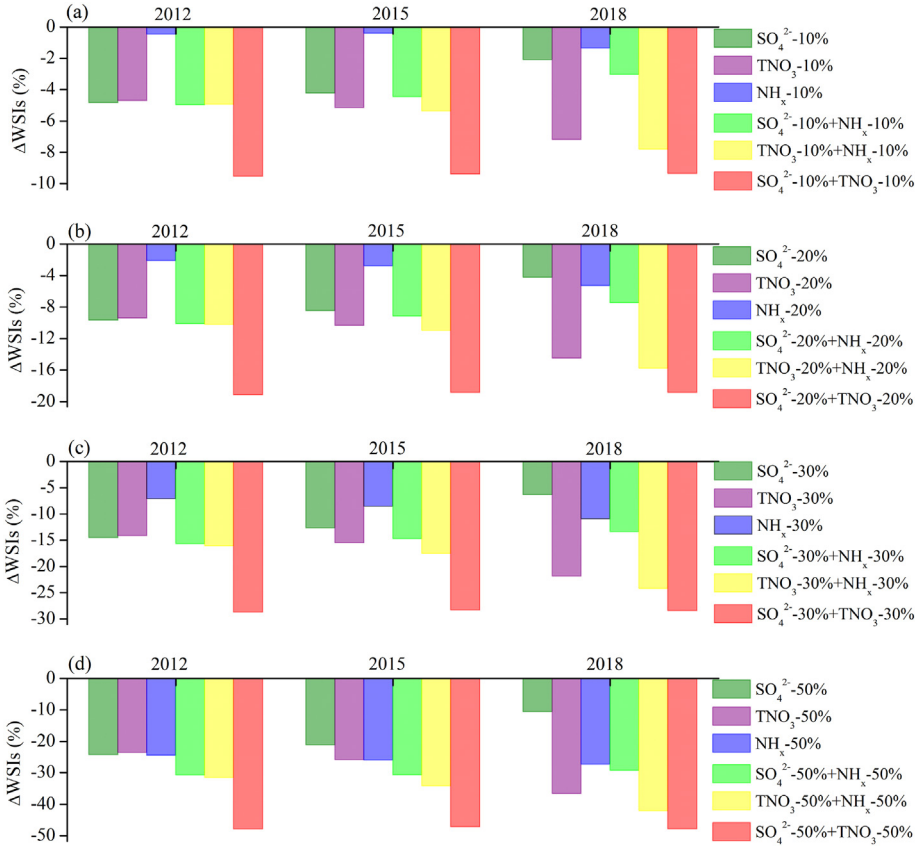

Fig. 6. WSIs reduction under the scenarios of 10%, 20%, 30% and 50% reduction of SO_4^{2-}, TNO_3, NH_x, and their combined reduction. The base scenario is no SO_4^{2-}, TNO_3 or NH_x reduction. WSIs including SO_4^{2-}, NO_3^-, NH_4^+, Cl^-, HSO_4^-, K^+, Na^+, Mg^{2+} and Ca^{2+}.

The observations we analyzed here show that inorganic $PM_{2.5}$ concentrations do not respond sensitively to the initial reduction of ammonia from 2012 to 2018. In this regime, considerations such as costs associated with different abatement strategies are not needed because the low cost of ammonia control will not lead to a corresponding decrease of inorganic $PM_{2.5}$. From a short-term perspective of $PM_{2.5}$ control, reducing SO_2 and NO_x is effective than reducing NH_3. From a long-term perspective, as emission reductions and other process lead to ammonia concentration approaching the CTAC point, a tendency of which was found in this study, ammonia control may become more effective for $PM_{2.5}$ abatement than the controls of SO_2 and NO_x. The CTAC analysis will assist the formulation of the $PM_{2.5}$ reduction strategies.

CRediT authorship contribution statement

Mingming Zheng: Methodology, Investigation, Formal analysis, Writing-original draft. **Yuhang Wang**: Writing-review & editing, Project administration. **Lianxin Yuan**: Resources, Validation. **Nan Chen**: Investigation, Data curation. **Shaofei Kong**: Writing-review & editing, Funding acquisition.

Declaration of competing interest

The authors declare that they have no known competing financial interests or personal relationships that could have appeared to influence the work reported in this paper.

Acknowledgements

This study was financially supported by the National Natural Science Fund (41830965), the Key Program of Ministry of Science and Technology of the People's Republic of China (2016YFA0602002; 2017YFC0212602), and the Key Program for Technical Innovation of Hubei Province (2017ACA089). Y. Wang was supported by the National Science Foundation. Funding was also provided by the Research and Innovation Initiatives of WHPU (2021Y17).

Appendix A. Supplementary data

Supplementary data to this article can be found online at https://doi.org/10.1016/j.scitotenv.2022.153708.

References

An, Z., Huang, R.J., Zhang, R., Tie, X., Li, G., Cao, J., Zhou, W., Shi, Z., Han, Y., Gu, Z., Ji, Y., 2019. Severe haze in Northern China: a synergy of anthropogenic emissions and atmospheric processes. Proc. Natl. Acad. Sci. 116 (18), 8657–8666.

Ansari, A.S., Pandis, S.N., 2000. The effect of metastable equilibrium states on the partitioning of nitrate between the gas and aerosol phases. Atmos. Environ. 34 (1), 157–168.

Backes, A.M., Aulinger, A., Bieser, J., Matthias, V., Quante, M., 2016. Ammonia emissions in Europe, part II: how ammonia emission abatement strategies affect secondary aerosols. Atmos. Environ. 126, 153–161.

Bai, Z., Winiwarter, W., Klimont, Z., Velthof, G., Misselbrook, T., Zhao, Z., Jin, X., Oenema, O., Hu, C., Ma, L., 2019. Further improvement of air quality in China needs clear ammonia mitigation target. Environ. Sci. Technol. 53, 10542–10544.

Behera, S.N., Sharma, M., 2010. Investigating the potential role of ammonia in ion chemistry of fine particulate matter formation for an urban environment. Sci. Total Environ. 408 (17), 3569–3575.

Bertram, A.K., Martin, S.T., Hanna, S.J., Smith, M.L., Bodsworth, A., Chen, Q., Kuwata, M., Liu, A., You, Y., Zorn, S.R., 2011. Predicting the relative humidities of liquid-liquid phase separation, efflorescence, and deliquescence of mixed particles of ammonium sulfate, organic material, and water using the organic-to-sulfate mass ratio of the particle and the oxygen-to-carbon elemental ratio of the organic component. Atmos. Chem. Phys. 11 (21), 10995–11006.

Blanchard, C., Rose, P., Tanenbaum, S., Ziman, S., Seinfeld, J., 2000. The use of ambient measurements to identify which precursor species limit aerosol nitrate formation. J. AirWaste Manag. Assoc. 50 (12), 2073–2084.

Cao, J., 2012a. Pollution status and control strategies of $PM_{2.5}$ in China. J. Earth Environ. 3, 1030–1036.

Cao, J.J., Shen, Z.X., Chow, J.C., Watson, J.G., Lee, S.C., Tie, X.X., Ho, K.F., Wang, G.H., Han, Y.M., 2012b. Winter and summer $PM_{2.5}$ chemical compositions in fourteen Chinese cities. J. AirWasteManag. Assoc. 62 (10), 1214–1226.

Cheng, J., Su, J., Cui, T., Li, X., Dong, X., Sun, F., Yang, Y., Tong, D., Zheng, Y., Li, Y., Li, J., Zhang, Q., He, K., 2019. Dominant role of emission reduction in $PM_{2.5}$ air quality improvementin Beijing during 2013–2017: a model-based decomposition analysis. Atmos. Chem. Phys. 6125–6146.

Cheng, L., Ye, Z., Cheng, S., Guo, X., 2021. Agricultural ammonia emissions and its impact on $PM_{2.5}$ concentrations in the Beijing-Tianjin-Hebei region from 2000 to 2018. Environ. Pollut. 291, 118162.

China State Council, 2013. Action plan on prevention and control of air pollution. http://www.gov.cn/zwgk/2013-09/12/content_2486773.htm. (Accessed 19 October 2020).

China State Council, 2017. Opinions of the General Office of the State Council on Accelerating the Resource Utilization of Livestock and Poultry Wastes. http://www.gov.cn/zhengce/content/2017-06/12/content_5201790.htm. (Accessed 10 March 2020).

China State Council, 2018. Three-year action plan for winning the blue sky defense battle. http://www.gov.cn/zhengce/content/2018-07/03/content_5303158.htm. (Accessed 9 October 2020).

Chu, B., Kerminen, V., Bianchi, F., Yan, C., Petäjä, T., Kulmala, M., 2019. Atmospheric new particle formation in China. Atmos. Chem. Phys. 19, 115–138.

Das, P., Sa, J., Kim, K., Jeon, E., 2009. Effect of fertilizer application on ammonia emission and concentration levels of ammonium, nitrate, and nitrite ions in a rice field. Environ. Monit. Assess. 154, 275–282.

Dennis, R.L., Bhave, P.V., Pinder, R.W., 2008. Observable indicators of the sensitivity of $PM_{2.5}$ nitrate to emission reductions-part II: sensitivity to errors in total ammonia and total nitrate of the CMAQ-predicted non-linear effect of SO_2 emission reductions. Atmos. Environ. 42, 1287–1300.

Fountoukis, C., Nenes, A., 2007. ISORROPIAII: a computationally efficient thermodynamic equilibrium model for K^+-Ca^{2+}-Mg^{2+}-NH_4^+-Na^+-SO_4^{2-}–NO_3^-–Cl^-–H_2O aerosols. Atmos. Chem. Phys. 7 (17), 4639–4659.

Fu, H., Chen, J., 2017. Formation, features and controlling strategies of severe haze-fog pollutions in China. Sci. Total Environ. 578, 121–138.

Fu, X., Wang, S., Xing, J., Zhang, X., Wang, T., Hao, J., 2017. Increasing ammonia concentrations reduce the effectiveness of particle pollution control achieved via SO_2 and NO_x emissions reduction in East China. Environ. Sci. Technol. Lett. 4 (6), 221–227.

Fu, X., Wang, T., Gao, J., Wang, P., Liu, M., Wang, S., Zhao, B., Xue, L., 2020. Persistent heavy winter nitrate pollution driven by increased photochemical oxidants in northern China. Environ. Sci. Technol. 54, 3881–3889.

Geng, G., Zhang, Q., Tong, D., Li, M., Zheng, Y., Wang, S., He, K., 2017. Chemical composition of ambient $PM_{2.5}$ over China and relationship to precursor emissions during 2005-2012. Atmos. Chem. Phys. 9187–9203.

Geng, G., Xiao, Q., Zheng, Y., Tong, D., Zhang, Y., Zhang, X., Zhang, Q., He, K., Liu, Y., 2019. Impact of China's air pollution prevention and control action plan on $PM_{2.5}$ chemical composition over eastern China. Sci. China Earth Sci. 62, 1872–1884.

Gu, B., Zhang, L., Dingenen, R., Vieno, M., Grinsven, H., Zhang, X., Zhang, S., Chen, Y., Wang, S., Ren, C., Rao, S., Holland, M., Winiwarter, W., Chen, D., Xu, J., Sutton, M., 2021. Abating ammonia is more cost-effective than nitrogen oxides for mitigating $PM_{2.5}$ air pollution. Science 374, 758–762.

Guo, H., Xu, L., Bougiatioti, A., Cerully, K.M., Capps, S.L., Hite Jr., J.R., Carlton, A.G., Lee, S.H., Bergin, M.H., Ng, N.L., Nenes, A., 2015. Fine-particle water and pH in the southeastern United States. Atmos. Chem. Phys. 15 (9), 5211–5228.

Guo, H., Sullivan, A.P., Campuzano-Jost, P., Schroder, J.C., Lopez-Hilfiker, F.D., Dibb, J.E., Jimenez, J.L., Thornton, J.A., Brown, S.S., Nenes, A., Weber, R.J., 2016. Fine particle pH and the partitioning of nitric acid during winter in the northeastern United States. J. Geophys. Res. Atmos. 121 (17), 10–355.

Guo, H., Liu, J., Froyd, K.D., Roberts, J.M., Veres, P.R., Hayes, P.L., Jimenez, J.L., Nenes, A., Weber, R.J., 2017. Fine particle pH and gas-particle phase partitioning of inorganic species in Pasadena, California, during the 2010 CalNex campaign. Atmos. Chem. Phys. 17 (9), 5703–5719.

Guo, H., Otjes, R., Schlag, P., Kiendler-Scharr, A., Nenes, A., Weber, R.J., 2018. Effectiveness of ammonia reduction on control of fine particle nitrate. Atmos. Chem. Phys. 18 (16), 12241–12256.

Hennigan, C.J., Izumi, J., Sullivan, A.P., Weber, R.J., Nenes, A., 2015. A critical evaluation of proxy methods used to estimate the acidity of atmospheric particles. Atmos. Chem. Phys. 15 (5), 2775–2790.

Huang, X., Song, Y., Li, M., Li, J., Huo, Q., Cai, X., Zhu, T., Hu, M., Zhang, H., 2012. A high-resolution ammonia emission inventory in China. Glob.Biogeochem. Cycles 26 (1).

Jin, Y., Andersson, H., Zhang, S., 2016. Air pollution control policies in China: a retrospective and prospects. Int.J. Environ. Res. Public Health 13 (12), 1219.

Li, M., Zhang, L., 2014. Haze in China: current and future challenges. Environ. Pollut. 189, 85–86.

Li, H., Wang, D., Cui, L., Gao, Y., Huo, J., Wang, X., Zhang, Z., Tan, Y., Huang, Y., Cao, J., Chow, J.C., 2019. Characteristics of atmospheric $PM_{2.5}$ composition during the implementation of stringent pollution control measures in Shanghai for the 2016 G20 summit. Sci. Total Environ. 648, 1121–1129.

Liu, M., Huang, X., Song, Y., Tang, J., Cao, J., Zhang, X., Zhang, Q., Wang, S., Xu, T., Kang, L., Cai, X., 2019. Ammonia emission control in China would mitigate haze pollution and nitrogen deposition, but worsen acid rain. Proc. Natl. Acad. Sci. 116 (16), 7760–7765.

Ma, R., Li, K., Guo, Y., Zhang, B., Zhao, X., Linder, S., Guan, C., Chen, G., Gan, Y., Meng, J., 2021. Mitigation potential of global ammonia emissions and related health impacts in the trade network. Nat. Commun. 12, 7084.

Murphy, J.G., Gregoire, P.K., Tevlin, A.G., Wentworth, G.R., Ellis, R.A., Markovic, M.Z., VandenBoer, T.C., 2017. Observational constraints on particle acidity using measurements and modelling of particles and gases. Faraday Discuss. 200, 379–395.

Nenes, A., Pandis, S.N., Pilinis, C., 1998. ISORROPIA: a new thermodynamic equilibrium model for multiphase multicomponent inorganic aerosols. Aquat. Geochem. 4 (1), 123–152.

Ou, J., Hu, Q., Liu, H., Xu, S., Wang, Z., Ji, X., Wang, X., Xie, Z., Kang, H., 2022. Exploring the impact of new particle formation events on $PM_{2.5}$ pollution during winter in the Yangtze River Delta, China. J. Environ. Sci. 111, 75–78.

Pan, D., Benedict, K.B., Golston, L.M., Wang, R., Collett, J.L., Tao, L., Sun, K., Guo, X., Ham, J., Prenni, A.J., Schichtel, B.A., Mikoviny, T., Müller, M., Wisthaler, A., Zondlo, M.A., 2021. Ammonia dry deposition in an alpine ecosystem traced to agricultural emission hotpots. Environ. Sci. Technol. 55, 7776–7785.

Pinder, R.W., Adams, P.J., Pandis, S.N., 2007. Ammonia emission controls as a cost-effective strategy for reducing atmospheric particulate matter in the eastern United States. Environ. Sci. Technol. 41, 380–386.

Pinder, R., Dennis, R., Bhave, P., 2008. Observable indicators of the sensitivity of $PM_{2.5}$ nitrate to emission reductions-part I: derivation of the adjusted gas ratio and applicability at regulatory-relevant time scales. Atmos. Environ. 42, 1275–1286.

Plautz, J., 2018. Piercing the haze. Science 1060–1063.

Seinfeld, J.H., Pandis, S.N., 2006. Atmospheric Chemistry And Physics: From Air Pollution to Climate Change. Third ed. John Wiley & Sons, Inc., Hoboken, New Jersey.

Song, S., Gao, M., Xu, W., Shao, J., Shi, G., Wang, S., Wang, Y., Sun, Y., McElroy, M.B., 2018. Fine-particle pH for Beijing winter haze as inferred from different thermodynamic equilibrium models. Atmos. Chem. Phys. 18 (10), 7423–7438.

Wang, S., Xing, J., Jang, C., Zhu, Y., Fu, J.S., Hao, J., 2011. Impact assessment of ammonia emissions on inorganic aerosols in East China using response surface modeling technique. Environ. Sci. Technol. 45 (21), 9293–9300.

Wang, J., Zhao, B., Wang, S., Yang, F., Xing, J., Morawska, L., Ding, A., Kulmala, M., Kerminen, V.M., Kujansuu, J., Wang, Z., 2017. Particulate matter pollution over China and the effects of control policies. Sci. Total Environ. 584, 426–447.

Wang, Y., Wang, Y., Wang, L., Petäjä, T., Zha, Q., Gong, C., Li, S., Pan, Y., Hu, B., Xin, J., Kulmala, M., 2019. Increased inorganic aerosol fraction contributes to air pollution and haze in China. Atmos. Chem. Phys. 19 (9), 5881–5888.

Weber, R.J., Guo, H., Russell, A.G., Nenes, A., 2016. High aerosol acidity despite declining atmospheric sulfate concentrations over the past 15 years. Nat. Geosci. 9 (4), 282–285.

Wu, Y., Gu, B., Erisman, J., Reis, S., Fang, Y., Lu, X., Zhang, X., 2016. $PM_{2.5}$ pollution is substantially affected by ammonia emissions in China. Environ. Pollut. 218, 86–94.

Xu, Z., Liu, M., Zhang, M., Song, Y., Wang, S., Zhang, L., Xu, T., Wang, T., Yan, C., Zhou, T., Sun, Y., Pan, Y., Hu, M., Zheng, M., Zhu, T., 2019. High efficiency of livestock ammonia emission controls in alleviating particulate nitrate during a severe winter haze episode in northern China. Atmos. Chem. Phys. 19, 5605–5613.

Yang, Y., Liao, H., Lou, S., 2016. Increase in winter haze over eastern China in recent decades: roles of variations in meteorological parameters and anthropogenic emissions. J. Geophys. Res. Atmos. 121, 13050–13065.

Zhang, X., Wu, Y., Liu, X., Reis, S., Jin, J., Dragosits, U., Van Damme, M., Clarisse, L., Whitburn, S., Coheur, P.F., Gu, B., 2017. Ammonia emissions may be substantially underestimated in China. Environ. Sci. Technol. 51 (21), 12089–12096.

Zhang, Q., Zheng, Y., Tong, D., Shao, M., Wang, S., Zhang, Y., Xu, X., Wang, J., He, H., Liu, W., Ding, Y., Lei, Y., Li, J., Wang, Z., Zhang, X., Wang, Y., Cheng, J., Liu, Y., Shi, Q., Yan, L., Geng, G., Hong, C., Li, M., Liu, F., Zheng, B., Cao, J., Ding, A., Gao, J., Fu, Q., Huo, J., Liu, B., Liu, Z., Yang, F., He, K., Hao, J., 2019. Drivers of improved $PM_{2.5}$ air quality in China from 2013 to 2017. Proc. Natl. Acad. Sci. 116, 24463–24469.

Zhang, Q., Pan, Y., He, Y., Walters, W., Ni, Q., Liu, X., Xu, G., Shao, J., Jiang, C., 2020. Substantial nitrogen oxides emission reduction from China due to COVID-19 and its impact on surface ozone and aerosol pollution. Sci. Total. Environ. 753.

Zhao, B., Wang, S.X., Liu, H., Xu, J.Y., Fu, K., Klimont, Z., Hao, J.M., He, K.B., Cofala, J., Amann, M., 2013. NOx emissions in China: historical trends and future perspectives. Atmos. Chem. Phys. 13 (19), 9869–9897.

Zheng, B., Tong, D., Li, M., Liu, F., Hong, C., Geng, G., Li, H., Li, X., Peng, L., Qi, J., Yan, L., Zhang, Y., Zhao, H., Zheng, Y., He, K., Zhang, Q., 2018. Trends in China's anthropogenic emissionssince 2010 as the consequence of clean air actions. Atmos. Chem. Phys. 14095–14111.

Zheng, M., Wang, Y., Bao, J., Yuan, L., Zheng, H., Yan, Y., Liu, D., Kong, S., 2019. Initial cost barrier of ammonia control in central China. Geophys. Res. Lett. 46 (23), 14175–14184.

Zhou, X., Strezov, V., Jiang, Y., Kan, T., Evans, T., 2022. Temporal and spatial variations of air pollution across China from 2015 to 2018. J. Environ. Sci. 112, 161–169.